Review Article

Permeability imaging in pediatric brain tumors

Sandi Lam[1], Yimo Lin[1], Peter C. Warnke[2]

[1]Department of Neurosurgery, Baylor College of Medicine, Texas Children's Hospital, Houston, Texas, USA; [2]Functional and Stereotactic Neurosurgery, Department of Surgery, University of Chicago, Chicago, Illinois, USA

Correspondence to: Sandi Lam, MD. Department of Neurosurgery, Baylor College of Medicine/Texas Children's Hospital, 6701 Fannin St, CCC 1230, Houston TX 77030, USA. Email: sandilam@gmail.com or sandi.lam@bcm.edu.

Abstract: While traditional computed tomography (CT) and magnetic resonance (MR) imaging illustrate the structural morphology of brain pathology, newer, dynamic imaging techniques are able to show the movement of contrast throughout the brain parenchyma and across the blood-brain barrier (BBB). These data, in combination with pharmacokinetic models, can be used to investigate BBB permeability, which has wide-ranging applications in the diagnosis and management of central nervous system (CNS) tumors in children. In the first part of this paper, we review the technical principles underlying four imaging modalities used to evaluate BBB permeability: PET, dynamic CT, dynamic T1-weighted contrast-enhanced MR imaging, and dynamic T2-weighted susceptibility contrast MR. We describe the data that can be derived from each method, provide some caveats to data interpretation, and compare the advantages and disadvantages of the different techniques. In the second part of this paper, we review the clinical applications that have been reported with permeability imaging data, including diagnosing the nature of a lesion found on imaging (neoplastic versus non-neoplastic, tumor type, tumor grade, recurrence versus pseudoprogression), predicting the natural history of a tumor, monitoring angiogenesis and tracking response to anti-angiogenic agents, optimizing chemotherapy agent selection, and aiding in the development of new antineoplastic drugs and methods to increase local delivery of chemotherapeutics.

Keywords: Permeability imaging; brain tumor imaging; MRI; positron emission tomography (PET); computed tomography (CT); pediatric brain tumor

Submitted Jul 01, 2014. Accepted for publication Jul 03, 2014.
doi: 10.3978/j.issn.2224-4336.2014.07.01
View this article at: http://dx.doi.org/10.3978/j.issn.2224-4336.2014.07.01

Introduction

The blood brain barrier (BBB) consists of tight-junction forming endothelial cells, pericytes, and astrocytes that form a barrier between the blood and the brain extracellular space. It is normally impermeable to all water-soluble substances except for those that have specialized transporters (i.e., glucose, amino acids), or substances that are very small (1). Various pathologies, such as abscess, necrosis, or tumor, as well as some therapies like ionizing radiation and heat, may lead to increased BBB permeability. This increase can be identified on a number of imaging modalities. Since computed tomography (CT) and magnetic resonance (MR) contrast agents typically do not cross a normal, intact BBB, contrast-enhancement of a region of brain parenchyma on static scans typically implies either increased permeability or increased vascular volume; the distinction can be made by kinetic analysis. PET imaging, as well as newer, dynamic methods of CT and MR imaging, allow this pharmacokinetic analysis by quantifying the movement of contrast from vessels into brain parenchyma. From these data, transport rates describing BBB permeability can be derived. Permeability data as measured by these dynamic imaging techniques can be used to predict drug delivery, identify areas of different tumor grade within a given neoplasm, predict the natural history of a lesion to guide aggressiveness of intervention, evaluate response to treatment, and many other clinically useful applications (2-10). Many groups have already begun using permeability imaging methods as a noninvasive tool

to aid in the management of neoplasms of the brain.

The goal of this review paper is to describe the dynamic imaging methods most commonly used to assess permeability in brain tumors and to review the clinical applications of these methods in pediatric and adult populations. First, this study will describe the principles underlying PET, dynamic CT, dynamic T1-weighted contrast-enhanced MR imaging, and dynamic T2-weighted susceptibility contrast MR, and will address the data that can be derived from each method as well as the comparative advantages and disadvantages. Second, this study will describe the clinical applications that have been reported with permeability imaging data, notably: (I) diagnosing the nature of a lesion found on imaging (neoplastic *vs.* non-neoplastic, tumor type, tumor grade, recurrence *vs.* pseudoprogression); (II) predicting the natural history of a tumor; (III) monitoring angiogenesis and tracking response to anti-angiogenic agents; (IV) optimizing chemotherapy agent selection and (V) aiding in the development of new antineoplastic drugs and methods to increase local delivery.

Measurement of blood-brain barrier (BBB) permeability

The permeability of the BBB is compound-specific and describes the velocity by which a molecule crosses the endothelial cell membrane separating the vascular compartment from the extracellular space. The process in place is passive diffusion and the driving force is the concentration gradient of the specific compound. Naturally, lipophilic compounds cross the lipid bilayer membrane more easily than hydrophilic compounds; the latter cross the cell membrane only to a minimal extent. The actual permeability surface-area product can be derived by measuring simultaneously the arterial concentration and the tissue concentration of a marker, and applying a two compartment model describing the kinetics of exchange between compartments. This is usually unidirectional given the excessive plasma concentration of the marker at the outset and the limited accumulation in the extracellular space during the time of the experiment.

The permeability for a given molecule depends on the octanol/water partition coefficient, the molecular weight, the hydraulic and electrical conductivity of the membrane and the osmotic reflection coefficient (11,12).

To quantify the passive transport of substances across the BBB, the concept of transfer rates was introduced. This concept is analogous to renal clearance rates that describe the volume of plasma that is theoretically cleared of the measured compound per unit time and per circulation cycle. This results in a transfer rate (K1) given in milliliters or microliters/100 grams/minute. These transfer rates were first measured using quantitative autoradiography (QAR) and radiolabeled compounds. To measure transfer rates, the arterial concentration of the radiolabel is measured continuously during and after rapid intravenous infusion and then integrated over time. Thus an arterial input function could be generated. The tissue concentration is then measured at the end of the experiment from actual tissue samples. Using a two compartment pharmacokinetic model (extracellular space and vascular space), the transport rates could then be calculated, deriving the tissue concentration as a function of the arterial input and transfer rates. QAR has been used widely to characterize the BBB function in brain tumor models (13-15). As a logical extension of QAR to measure tissue concentration non-invasively, positron emission tomography (PET) employing rubidium-82 and 68-Ga-EDTA (gallium, ethylenediaminetetraacetic acid) have been used to measure K1. This technique uses the same principles as QAR but measures the tissue concentration of the positron-emitter labeled compound from the radioactive signal, rather than from tissue samples.

Imaging methods

Positron emission tomography (PET)

The kinetics of tissue distribution of a given compound of interest can be measured by attaching positron-emitting isotopes (like F-18) to the compound, injecting it into a subject, and quantifying the radioactive signal from a region of interest (i.e., the brain), correcting for any radioactive decay that occurs during the experiment. The arterial input integral is obtained from serial measurements of the marker concentration in arterial samples. The PET system detects pairs of gamma-rays emitted by the isotope, and reconstructs a three-dimensional image of the local concentrations of the positron emitter. The major advantage of PET is that numerous compounds of interest, including most drugs of interest in pediatric brain tumors as well as biological compounds such as monoclonal antibodies, can be labeled with positron emitters like F-18, C-11 or J-124. The disadvantage of PET stems from its limited spatial resolution, the high cost involved with the use of radionuclides and the exposure to whole body radiation, particularly in sequential studies.

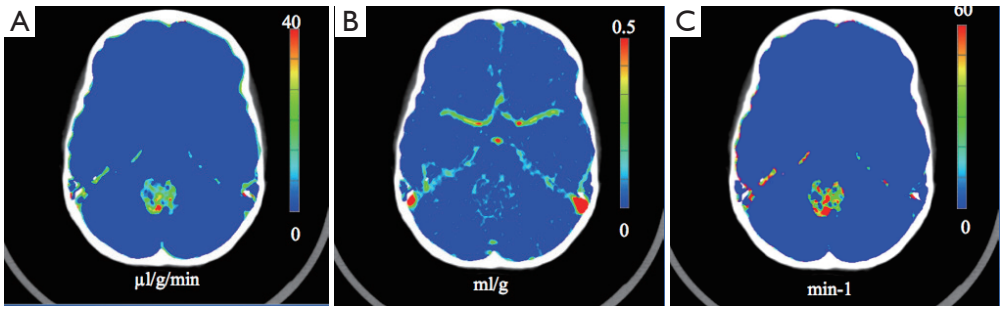

Figure 1 (A) CT measurement of capillary permeability. Quantitative image of blood-to-brain transport rate in an untreated medulloblastoma. The color bar refers to quantitative values in microliters/gram/minute. Note the heterogeneous distribution of permeability values within the tumor resulting in up to 10-fold differences in permeability in even adjacent tumor areas; (B) quantitative image of plasma vascular space; (C) regional distribution of brain efflux constant k2.

Dynamic CT

CT measurements of capillary permeability were introduced by Groothuis *et al.* and validated against measurements in the same experimental subject at identical positions with QAR (16). Standard CT contrast agents can be used to measure permeability. The iodine content, which is linearly related to the Hounsfield units describing X-ray attenuation, is measured to derive simultaneous arterial and tissue concentrations. The arterial concentration can be derived non-invasively from serial scanning over a major cerebral artery and calculating the change in Hounsfield number after pre-contrast background subtraction. Using a modified Patlak-plot, the input for the compartment models can then be generated.

By fitting the data to a two-compartment model, both permeability information as well as the size of the vascular volume can be derived (*Figure 1A,B*) (3-5). Furthermore, by scanning up to 30 minutes after cessation of the intravenous marker infusion, the efflux constant or brain to blood transfer constant k2 (in reciprocal time) which describes how rapidly the marker diffuses back into the vascular compartment, can be measured, giving full kinetic information (*Figure 1C*). If a marker is used that only distributes in the extracellular space and does not enter the cell parenchyma, the ratio k1/k2 actually represents the distribution space in a tumor—that is, the extracellular space of a given tumor. One caveat of this technique is that the derived relative cerebral blood volume (rCBV) values can be overestimated in tumors with high permeability, in particular lymphomas, as early crossing of the marker into the extracellular space mimics filling of the vascular compartment. This is superimposed on the vascular component of the rapid phase of the concentration/signal curve and needs to be corrected for (3-5).

Advantages of the dynamic CT technique are that it is fast, economical, and utilizes equipment found in most hospitals. Additionally, unlike with MR, in CT imaging there exists a linear relationship between contrast concentration and signal intensity; combined with an arterial input function, even absolute values for blood flow may be calculated. The most significant disadvantage of this technique is the radiation exposure, given the increased number of scans per session and the use of continuous scanning. The method described by Jain involved a total of 170 seconds of acquisition time, significantly more than a standard head CT (3). Finally, as children with central nervous system (CNS) tumors are typically followed by MRI, the use of perfusion CT would necessitate additional scans, with concomitant contrast exposure, radiation exposure, and cost.

Dynamic contrast-enhanced MRI

T1-weighted Dynamic Contrast-Enhanced (DCE) Imaging is another method used to perform “permeability imaging”. In conventional MR, a paramagnetic contrast agent is injected, some time passes, a brain image is taken, and the presence of contrast-enhancing lesions will be appreciated by changes in the T1 image; however this is a static picture in time. With DCE, the same contrast is injected and is immediately followed by a series of fast T1-weighted MR images. This process allows for visualization of the contrast as it moves through the vasculature and extravasates from the intravascular space into areas of brain parenchyma with altered permeability (17-19). Changes in the signal

intensity, compared to a non-contrast baseline image, can be used to approximate contrast concentrations within the varying compartments after correction for vascular space, the other contributor to T1 changes; these data can then be fed into a pharmacokinetic two-compartment model and integrated over time to determine the unidirectional movement of contrast (17,20). From these data, it is possible to derive a rate constant of the transfer from the intravascular to the interstitial space (Ktrans or K1) and the volume of the intravascular space corrected for hematocrit. Unlike in CT, the concentration to signal relation in MR is non-linear, which requires application of non-linear mathematical solutions. Some other caveats of this method include the following: Ktrans is a constant that describes movement between two compartments separated by a cell membrane. Under conditions of high blood flow and low permeability where the limiting factor for transcapillary transport is permeability, Ktrans approaches permeability surface area product per unit volume of tissue. In the rare scenario when blood flow is slow, movement across the barrier will be perfusion-limited, and Ktrans may underestimate permeability (6,19). Other factors may affect the permeability of a given molecule, such as the hydraulic conductivity and the osmotic reflection coefficient (6,19). As well, it is critical to differentiate the intravascular from the extravascular-extracellular space; the mathematical models assume that the initial fast slope of enhancement of a given voxel represents intravascular contrast, and any enhancement occurring later in time in that voxel represents extravasation. This may both downplay or overrate the contribution of the intravascular compartment and over/underestimate Ktrans, particularly in tumors without a BBB where the tissues fill with contrast at the same rate as the vasculature, like meningiomas or primary CNS lymphomas (17-19).

However, despite these limitations, Jackson *et al.* (n=9) showed that Ktrans values derived from this imaging modality were reproducible at two different timepoints in a population of people with newly-diagnosed glioma (21). Calculated Ktrans values are highly dependent on the pharmacokinetic model and image acquisition parameters used, thus rendering comparison of values published by different groups difficult.

Advantages of this method are that it allows the quantitative evaluation of BBB integrity and microvascular permeability, and there exists a sizeable amount of published data with clinical correlates for this technique. Specific advantages over T2-weighted dynamic susceptibility contrast (DSC) MR imaging include higher spatial resolution, lower contrast dose, and lack of vulnerability to susceptibility artifact from bone, blood, air, calcification, or metal (7,17,18). Additionally, DCE is designed to measure tissue permeability: the data is obtained when the contrast reaches a steady-state equilibrium in the tissue, and the mathematical models used to calculate Ktrans account for contrast extravasation across the BBB. On the other hand, DSC is typically used to obtain perfusion data, and thus only examines the first-pass of the contrast through the vasculature and uses mathematical models that assume that all of the injected contrast remains in the intravascular compartment. Permeability constants can be calculated from DSC data using different models (that do not assume the contrast remains intravascular), but they will still be based on first-pass data, which may not reflect the true permeability of the tissue. Empirically, permeability values from DSC do not always correlate with those derived from T1-DCE methods (17). An advantage of both MR techniques over dynamic CT is the lack of radiation exposure.

A major disadvantage of all dynamic imaging modalities is that they require the injection of a large bolus of contrast over a relatively short period of time, frequently necessitating power injectors and stable, large-bore IV access which may be difficult to attain in small children (7,9,22). The disadvantage of T1-DCE compared to DSC is longer imaging times, which leads to more risk for motion artifact and lower temporal resolution (18,22).

Dynamic susceptibility contrast imaging

T2-weighted DSC is a method traditionally referred to as "bolus-tracking" or "perfusion" imaging. It is primarily used to examine cerebral perfusion and to determine rCBV, however Ktrans values can be calculated from DSC data (17). Whereas in T1-DCE, the brain is imaged until the contrast reaches steady state levels after several minutes; T2-DSC aims to only look at the first-pass of the contrast through the tissues. After injection of contrast, a series of fast T2 or T2* echo planar MR images are taken, typically for only 60 seconds (6,7,18,23). These data can be mathematically processed to generate maps of rCBV, relative cerebral blood flow (rCBF) and permeability (Ktrans) (6,22). Cha *et al.* in a study published in 2006 (n=34) compared Ktrans values derived from T1-DCE and T2*-DSC methods, and found a strong correlation between the two among gliomas, but not meningiomas (17).

Caveats of this method include that DSC only measures permeability during the first pass of contrast, which is

likely to be different from what would be measured at steady state. This is problematic because the mathematical models from which Ktrans values are typically derived assume the bidirectional movement of contrast between two compartments, which may not be true in the first pass (6,17,20). Any delayed permeability will not be captured by this method; this is particularly relevant for tumors that are relatively impermeable or tumors that have relatively slower blood flow, perhaps due to extreme vessel tortuosity as is often seen in high-grade gliomas (6,17). As shown by Cha *et al.* above, Ktrans values derived from DSC data may not be accurate in cases of highly permeable tumors.

One advantage of the DSC method is the simultaneous derivation of rCBV data, which is widely used in the evaluation of brain tumors and has been shown to correlate with clinically useful information, such as tumor grade, aggressiveness, and prognosis (7,9,17,18,22-24). Additionally, compared to DCE, DSC imaging is faster, leading to less motion artifact and higher temporal resolution (17,18).

Disadvantages of the DSC method compared to DCE include the requirement of much more contrast injected at an even higher rate (3-5 mL/second); stable intravenous access of a sufficient caliber to attain these infusion rates may be difficult to attain in very young children. Additionally, DSC imaging has lower spatial resolution and is more vulnerable to susceptibility artifact, leading to poorer imaging of tissue near bone, calcifications, air, metal, or blood products, such as skull base or infratentorial tumors, tumors near large vessels, or hemorrhagic post-surgical cavities (7,18).

Overall MR-techniques employed to measure capillary permeability mostly report relative numbers of Ktrans/K1. Thorough validation against CT and PET quantitative data is still lacking.

All techniques of *in vivo* imaging of capillary permeability in pediatric brain tumors are plagued by a source of error: patient movement during the scanning. This leads to voxel shifts, resulting in possibly major errors in the calculated parameters. MR is the most sensitive to these errors due to the high spatial resolution. One solution that can be applied in patients that have to undergo a stereotactic procedure for clinical reasons is to perform the measurements under stereotactic conditions, with the head fixed in a stereotactic frame (25). This also solves the second inherent problem of *in vivo* imaging when sequential measurements in subjects is performed (for example, to quantify treatment effects): in order to assure that measurements are taken from exactly the same regions, parameter images need to be stereotactically reformatted and fused with the first set of measurements. This can be done with thin-slice acquisitions and image fusion or with repeated stereotactic measurements.

Clinical applications of permeability imaging

Differentiate neoplastic from non-neoplastic lesions

Dynamic imaging modalities have been used to differentiate neoplastic from non-neoplastic lesions in the brain. Jain *et al.* reported in a 2010 study (n=29) that perfusion CT can be used to differentiate tumefactive demyelinating lesions (TDL) from high-grade gliomas, as TDLs show statistically significantly lower permeability and perfusion on Dynamic CT (4). Haris *et al.* in a 2008 study (n=103) using DCE MR to differentiate infective lesions from glioma found that Ktrans values were able to correctly differentiate 98% of the high grade gliomas, 76% of the low grade gliomas, and 89% of the infectious lesions (26). It is important to realize that permeability values in a given tumor are heterogeneously distributed. Intratumoral physiological heterogeneity can be high, particularly in tumors such as GBM, so maintaining spatial resolution is important.

Differentiate gliomas from other tumors

Since extra-axial CNS tumors, metastases, and lymphomas recruit cerebral endothelial cells from the brain but sometimes induce fewer endothelial junctions, they can be much more permeable than intrinsic parenchymal neoplasms like gliomas. This fact can be used to differentiate these two categories of tumor by dynamic MR and CT imaging modalities. Because most calculations of rCBV assume that the contrast remains entirely intravascular, while calculations of Ktrans inherently account for the extravasation of contrast into tissues, Ktrans is a more reliable measurement in leaky tumors (17,18,27). Warnke *et al.* in a 2005 study (n=7) and a 2006 study (n=7) using dynamic CT to study tumor permeability found that CNS lymphomas had a blood-to-tissue transfer coefficient of 29.5 μL/gm/min, statistically significantly higher than metastases (16.5 μL/gm/min), anaplastic astrocytoma (12.3 μL/gm/min), glioblastoma multiforme (GBM) (11.2 μL/gm/min) and medulloblastoma (10.5 μL/gm/min) (10,28). Zhu *et al.* in a study (n=15) utilizing DCE found that measurements of leakage space were significantly larger in acoustic schwannomas than

meningiomas, which were in turn significantly larger than gliomas; histological studies have corroborated these findings (29,30).

Determine glioma grade

Many groups have published studies showing a correlation between permeability data derived from dynamic imaging and histologic grade among gliomas. Roberts *et al.* found in a study using T1-DCE imaging of 22 patients with gliomas (age range 14-79) that permeability correlated strongly (r=0.83) with tumor grade, even more strongly than fractional blood volume measurements (31). Jia *et al.* using the same technique (n=67 low and high grade astrocytomas) found that Ktrans and Ve values derived from T1-DCE were able to differentiate between grade II and grade III/IV astrocytomas, but not between grade III and grade IV tumors (32). The same group, in a different study (n=65) found that Ktrans and Ve were able to clearly distinguish between low grade (grade II) and anaplastic (grade III) oligodendrogliomas (33). Accurately distinguishing grade II from grade III tumors is important because the clinical management of low- and high-grade gliomas is different, with the latter typically receiving aggressive regimens of chemotherapy and radiation. Permeability imaging may be able to differentiate these two classes of tumors as low-grade gliomas rely on blood supply from native vessels with intact BBBs, and a hallmark of transition to a high-grade glioma is the secretion of neoangiogenic agents (like VEGF) which drive the creation of immature, leaky blood vessels (34). Cha *et al.* in a study of 20 low and high grade gliomas and 7 meningiomas found that Ktrans values derived from T1-DCE and T2*-DSC correlated strongly with each other in gliomas, but not in meningiomas. Ktrans was able to distinguish only between grade III and grade IV gliomas, but not between grade II and grade III; however there were only 5 grade II and 4 grade III patients in their study, so there were limitations associated with small sample size (17). Provenzale *et al.* in a study using T2*-DSC (n=22, age range, 26-75) found that Ktrans was able to differentiate between high grade (WHO grade 3 & 4) and low grade (WHO grade 1 & 2) gliomas, as the former were significantly more permeable. On the other hand, Law *et al.*, in a study of 73 patients with glioma (age 4-85) using T2*-DSC imaging and first-pass pharmacokinetic modeling to derive Ktrans values, found that rCBV correlated much more strongly with glioma grade than did Ktrans (6). In their study, regions of maximal rCBV and regions of maximal permeability shown on imaging maps did not always overlap. They postulate a theory that Ktrans and rCBV may be measuring different aspects of tumor physiology and development, specifically that Ktrans may be elevated in the initial stages of tumor angiogenesis, when vascular endothelial growth factor (VEGF) is stimulating the development of immature, leaky blood vessels, but that as the vessels mature, the BBB may become more robust, causing Ktrans to fall even though overall microvascular density and blood flow continue to increase. It is important to realize that permeability values in a given tumor are heterogeneously distributed. Intratumoral physiological heterogeneity can be high, particularly in tumors such as GBM, so spatial resolution is important. Finally, in a study using perfusion CT (n=32), Jain *et al.* found that both permeability and CBV data were able to clearly differentiate between high and low grade gliomas, and that permeability data was better at differentiating grade III from IV gliomas (35).

Differentiate pseudoprogression from recurrence

Accurately distinguishing radiation-induced necrosis from tumor recurrence is important, given the differences in clinical management. However this task can be very difficult with static imaging, as these two entities are often very similar in appearance. Currently, a definitive diagnosis requires histopathologic sampling, but dynamic imaging may provide a much less invasive method in the future. Jain *et al.* were able to demonstrate in a study using perfusion CT (n=38) that permeability measurements were clearly able to distinguish radiation necrosis from tumor recurrence (5). Barajas *et al.* found that measures of BBB integrity obtained from T1-DCE MR imaging were able to distinguish tumor recurrence from radiation necrosis after gamma-knife radiosurgery (36) as well as external beam radiotherapy (37). Shin *et al.* found in a study of 31 glioma patients that Ktrans values derived from DCE were able to distinguish between recurrences and treatment-related changes (38).

Predict the natural history of a neoplasm

A method of predicting the natural history of a neoplasm would be an invaluable addition to the armamentarium of cancer treatment. It would allow patients to avoid unnecessary toxicity from treating lesions that would never have progressed and would also ensure sufficient treatment of aggressive cancers. While no method exists

that is able to perfectly predict outcomes, there is some evidence that permeability imaging can provide useful data about the natural history of a lesion. Jost *et al.* in a study of 27 children with optic pathway gliomas showed that permeability data derived from T1-DCE imaging was able to differentiate between clinically aggressive and clinically stable neoplasms (39). In this study, "clinically aggressive" was defined as a neoplasm that was deemed by a multidisciplinary care team to require intervention with surgery, chemotherapy, or radiation, and "stable" as not requiring any management. Jensen *et al.* (n=16 glioma patients, age range, 19-79) reported a significant correlation between Ve (interstitial volume) data derived from T1-DCE and overall survival (40). Yang *et al.* (n=22) found that Ktrans data acquired from DCE-MR was able to differentiate between typical, benign meningiomas and the much more clinically aggressive and invasive atypical meningiomas (27). As well, Bhujwalla *et al.* reported a significant correlation between tumor permeability (T1-DCE) and metastatic propensity in cancer xenograft rodent models (41).

Monitor angiogenesis & response to anti-angiogenic agents

During the early stages of growth, astrocytomas subsist on blood flow from endogenous capillaries in the brain, and are thus limited in how large and how quickly they are able to grow (34). Developing the means to promote neoangiogenesis is a necessary step in the transformation of small, sub-mm tumors into large, rapidly growing, metastatic, clinically significant neoplasms (42-46). This process is referred to by many as the "angiogenic switch". Because the vessels produced by this process are leakier than the vessels in normal brain tissue, permeability imaging can be used to track the development of angiogenesis, and in the same way, to follow response to anti-angiogenic agents (8,22).

Studies have validated the utility of Ktrans as a proxy/biomarker for angiogenesis, reporting direct correlations between Ktrans, VEGF activity, and tumor growth in *in vitro* and *in vivo* models. Machein *et al.* in a study of 11 glioma subjects found that dynamic CT-derived permeability constants correlated with VEGF mRNA expression in tumor biopsy specimens (47). Bhujwalla *et al.* found that the application of an anti-angiogenic agent (TNP-470) in a cancer cell line led to decreases in both VEGF levels and dynamic-MR measured permeability (2). Raatschen *et al.* found that the application of an anti-VEGF drug in a cancer xenograft mouse model decreased both vessel permeability (seen on dynamic MR) and tumor growth rate (48). Pham *et al.* reported similar findings in a similar study (49), as did Brasch *et al.* (50) Gossman *et al.* saw a reduction in tumor permeability after the application of an anti-VEGF antibody in a xenograft glioma mouse model (51).

Permeability imaging has also been used to track response to anti-angiogenic therapy in human trials. In a phase II clinical trial of 16 patients with recurrent GBM, T1-DCE imaging was used to demonstrate vessel normalization and reduced vasogenic edema (corroborated with FLAIR imaging) after administration of a pan-VEGF receptor inhibitor (52). DCE derived Ktrans data was also used to track changes in vascular permeability in two phase II clinical trials of bevacizumab and irinotecan in pediatric patients with recurrent ependymoma and recurrent glioma/brainstem glioma (53,54). In both trials, DCE showed decreased permeability and a resultant minor reduction in edema after the administration of bevacizumab. Ultimately, both trials failed to show a survival benefit with the irinotecan/bevacizumab combination, however the DCE data may provide some insight into why. The changes in permeability that were seen were neither significant nor sustained, leading the authors to hypothesize that compensatory angiogenic mechanisms may have been at play, counteracting any survival benefit that would have been conferred by the bevacizumab.

All of these data suggest that permeability imaging may be an effective way to track response to anti-angiogenic chemotherapy regimens, and may even function as a tool to help develop newer and more effective anticancer drugs.

Optimize chemotherapy

Chemotherapy agents are only effective if they are able to reach the tumor; thus permeability is an important factor in the success of anti-cancer treatment. Warnke *et al.* showed that both capillary permeability and blood flow were low in medulloblastomas, potentially explaining the limited response to both hydrophilic and lipophilic chemotherapy agents that is seen in some patients (28). In a different study, the same group found high capillary permeability and blood flow in CNS lymphomas, which are known to be highly sensitive to hydrophilic chemotherapy agents (10). Blanchette *et al.* recently published a study showing that T1-DCE can be used to quantify drug movement across the BBB, laying the foundation for predicting drug delivery as a function of molecular size/weight and intrinsic BBB permeability (55). There also exist other preliminary data suggesting that permeability imaging may be able to be used to predict the ability of specific chemotherapy agents

to cross the BBB and enter a tumor (56).

Aid in the development of new anti-tumor agents

Many groups have proposed methods to selectively increase tumor permeability to facilitate the penetration and thus the effectiveness of anti-tumor agents (9,57-60). Permeability imaging modalities can be used as a tool to aid in the development of such methods. Intra-arterial infusion of hyperosmolar agents has been proposed as one way to temporarily permeabilize the BBB in order to increase delivery of water-soluble agents to tumors (60). The proposed mechanism is the osmotic shrinking of endothelial cells and subsequent opening of the junctions between them (9). Zünkeler *et al.* reported using PET-derived-permeability data in a baboon study (n=18) to show that intraarterial mannitol injections were able to significantly increase BBB permeability in a dose-dependent manner (60). On the other hand, Warnke *et al.* found that in ENU-induced gliomas, hyperosmotic infusions increased permeability in the surrounding normal brain but not in the tumor itself (15). Chemical modification of the BBB selectively in tumors using synthetic bradykinins has been employed successfully in experimental and human gliomas (61). Another method of selectively permeabilizing a section of BBB is with focused ultrasound and injected microbubbles; this method is currently under active study in rodent models (62-64). Yang *et al.* published data showing that DCE MR can monitor for BBB permeability changes induced by focused ultrasound, as Ktrans values correlated strongly with degree of Evans blue extravasation in rodent brain tissues (R=0.95) (65). Viachos reported similar findings in a similar experiment (66). Park *et al.* used T1-DCE to monitor the delivery of the chemotherapy agent doxorubicin across the BBB after permeabilization by focused ultrasound, and found a linear correlation between the doxorubicin concentration and the Ktrans value measured after sonication (56). All of these data suggest that permeability imaging may be a useful tool in the development of new treatments for CNS neoplasms.

Conclusions

Permeability imaging can be achieved with a number of different imaging modalities, including CT, PET and MRI. The applications of these methods in the diagnosis and management of pediatric CNS tumors is wide ranging. Research in this field is ongoing and actively evolving as clinicians find newer and more innovative applications for this technology.

Acknowledgements

None.

Footnote

Conflicts of Interest: PC Warnke is the Associate Editor of the *Journal of Neurology, Neurosurgery, and Psychiatry*. The other authors have no conflicts of interest to declare.

References

1. Levin VA. Relationship of octanol/water partition coefficient and molecular weight to rat brain capillary permeability. J Med Chem 1980;23:682-4.
2. Bhujwalla ZM, Artemov D, Natarajan K, et al. Reduction of vascular and permeable regions in solid tumors detected by macromolecular contrast magnetic resonance imaging after treatment with antiangiogenic agent TNP-470. Clin Cancer Res 2003;9:355-62.
3. Jain R. Perfusion CT imaging of brain tumors: an overview. AJNR Am J Neuroradiol2011;32:1570-7.
4. Jain R, Ellika S, Lehman NL, et al. Can permeability measurements add to blood volume measurements in differentiating tumefactive demyelinating lesions from high grade gliomas using perfusion CT? J Neurooncol 2010;97:383-8.
5. Jain R, Narang J, Schultz L, et al. Permeability estimates in histopathology-proved treatment-induced necrosis using perfusion CT: can these add to other perfusion parameters in differentiating from recurrent/progressive tumors? AJNR Am J Neuroradiol 2011;32:658-63.
6. Law M, Yang S, Babb JS, et al. Comparison of cerebral blood volume and vascular permeability from dynamic susceptibility contrast-enhanced perfusion MR imaging with glioma grade. AJNR Am J Neuroradiol 2004;25:746-55.
7. Poussaint TY, Rodriguez D. Advanced neuroimaging of pediatric brain tumors: MR diffusion, MR perfusion, and MR spectroscopy. Neuroimaging Clin N Am 2006;16:169-92, ix.
8. Provenzale JM, Mukundan S, Dewhirst M. The role of blood-brain barrier permeability in brain tumor imaging and therapeutics. AJR Am J Roentgenol 2005;185:763-7.
9. Rebeles F, Fink J, Anzai Y, et al. Blood-brain barrier imaging and therapeutic potentials. Top Magn Reson Imaging 2006;17:107-16.

10. Warnke PC, Timmer J, Ostertag CB, et al. Capillary physiology and drug delivery in central nervous system lymphomas. Ann Neurol 2005;57:136-9.
11. Rapoport SI. Factors which determine cerebrovascular permeability in the normal brain and following osmotic treatment. Adv Exp Med Biol 1980;131:179-92.
12. Smith QR, Momma S, Aoyagi M, et al. Kinetics of neutral amino acid transport across the blood-brain barrier. J Neurochem 1987;49:1651-8.
13. Groothuis DR, Warkne PC, Molnar P, et al. Effect of hyperosmotic blood-brain barrier disruption on transcapillary transport in canine brain tumors. J Neurosurg 1990;72:441-9.
14. Molnár PP, O'Neill BP, Scheithauer BW, et al. The blood-brain barrier in primary CNS lymphomas: ultrastructural evidence of endothelial cell death. Neuro Oncol 1999;1:89-100.
15. Warnke PC, Blasberg RG, Groothuis DR. The effect of hyperosmotic blood-brain barrier disruption on blood-to-tissue transport in ENU-induced gliomas. Ann Neurol 1987;22:300-5.
16. Groothuis DR, Lapin GD, Vriesendorp FJ, et al. A method to quantitatively measure transcapillary transport of iodinated compounds in canine brain tumors with computed tomography. J Cereb Blood Flow Metab 1991;11:939-48.
17. Cha S, Yang L, Johnson G, et al. Comparison of microvascular permeability measurements, K(trans), determined with conventional steady-state T1-weighted and first-pass T2*-weighted MR imaging methods in gliomas and meningiomas. AJNR Am J Neuroradiol 2006;27:409-17.
18. Essig M, Shiroishi MS, Nguyen TB, et al. Perfusion MRI: the five most frequently asked technical questions. AJR Am J Roentgenol 2013;200:24-34.
19. Kassner A, Roberts TP. Beyond perfusion: cerebral vascular reactivity and assessment of microvascular permeability. Top Magn Reson Imaging 2004;15:58-65.
20. Tofts PS, Kermode AG. Measurement of the blood-brain barrier permeability and leakage space using dynamic MR imaging. 1. Fundamental concepts. Magn Reson Med 1991;17:357-67.
21. Jackson A, Jayson GC, Li KL, et al. Reproducibility of quantitative dynamic contrast-enhanced MRI in newly presenting glioma. Br J Radiol 2003;76:153-62.
22. Lacerda S, Law M. Magnetic resonance perfusion and permeability imaging in brain tumors. Neuroimaging Clin N Am 2009;19:527-57.
23. Rossi A, Gandolfo C, Morana G, et al. New MR sequences (diffusion, perfusion, spectroscopy) in brain tumours. Pediatr Radiol 2010;40:999-1009.
24. Roberts HC, Roberts TP, Lee TY, et al. Dynamic contrast-enhanced computed tomography (CT) for quantitative estimation of microvascular permeability in human brain tumors. Acad Radiol 2002;9 Suppl 2:S364-7.
25. Behrens PF, Ostertag CB, Warnke PC. Regional cerebral blood flow in peritumoral brain edema during dexamethasone treatment: a xenon-enhanced computed tomographic study. Neurosurgery 1998;43:235-40; discussion 240-1.
26. Haris M, Gupta RK, Singh A, et al. Differentiation of infective from neoplastic brain lesions by dynamic contrast-enhanced MRI. Neuroradiology 2008;50:531-40.
27. Yang S, Law M, Zagzag D, et al. Dynamic contrast-enhanced perfusion MR imaging measurements of endothelial permeability: differentiation between atypical and typical meningiomas. AJNR Am J Neuroradiol 2003;24:1554-9.
28. Warnke PC, Kopitzki K, Timmer J, et al. Capillary physiology of human medulloblastoma: impact on chemotherapy. Cancer 2006;107:2223-7.
29. Long DM. Vascular ultrastructure in human meningiomas and schwannomas. J Neurosurg 1973;38:409-19.
30. Zhu XP, Li KL, Kamaly-Asl ID, et al. Quantification of endothelial permeability, leakage space, and blood volume in brain tumors using combined T1 and T2* contrast-enhanced dynamic MR imaging. J Magn Reson Imaging 2000;11:575-85.
31. Roberts HC, Roberts TP, Brasch RC, et al. Quantitative measurement of microvascular permeability in human brain tumors achieved using dynamic contrast-enhanced MR imaging: correlation with histologic grade. AJNR Am J Neuroradiol 2000;21:891-9.
32. Jia ZZ, Geng DY, Liu Y, et al. Microvascular permeability of brain astrocytoma with contrast-enhanced magnetic resonance imaging: correlation analysis with histopathologic grade. Chin Med J (Engl) 2013;126:1953-6.
33. Jia Z, Geng D, Liu Y, et al. Low-grade and anaplastic oligodendrogliomas: differences in tumour microvascular permeability evaluated with dynamic contrast-enhanced magnetic resonance imaging. J Clin Neurosci 2013;20:1110-3.
34. Young GS. Advanced MRI of adult brain tumors. Neurol Clin 2007;25:947-73, viii.
35. Jain R, Ellika SK, Scarpace L, et al. Quantitative estimation of permeability surface-area product in astroglial brain tumors using perfusion CT and correlation

with histopathologic grade. AJNR Am J Neuroradiol 2008;29:694-700.
36. Barajas RF, Chang JS, Sneed PK, et al. Distinguishing recurrent intra-axial metastatic tumor from radiation necrosis following gamma knife radiosurgery using dynamic susceptibility-weighted contrast-enhanced perfusion MR imaging. AJNR Am J Neuroradiol 2009;30:367-72.
37. Barajas RF Jr, Chang JS, Segal MR, et al. Differentiation of recurrent glioblastoma multiforme from radiation necrosis after external beam radiation therapy with dynamic susceptibility-weighted contrast-enhanced perfusion MR imaging. Radiology 2009;253:486-96.
38. Shin KE, Ahn KJ, Choi HS, et al. DCE and DSC MR perfusion imaging in the differentiation of recurrent tumour from treatment-related changes in patients with glioma. Clin Radiol 2014;69:e264-72.
39. Jost SC, Ackerman JW, Garbow JR, et al. McKinstry, Diffusion-weighted and dynamic contrast-enhanced imaging as markers of clinical behavior in children with optic pathway glioma. Pediatr Radiol 2008;38:1293-9.
40. Jensen RL, Mumert ML, Gillespie DL, et al. Preoperative dynamic contrast-enhanced MRI correlates with molecular markers of hypoxia and vascularity in specific areas of intratumoral microenvironment and is predictive of patient outcome. Neuro Oncol 2014;16:280-91.
41. Bhujwalla ZM, Artemov D, Natarajan K, et al. Vascular differences detected by MRI for metastatic versus nonmetastatic breast and prostate cancer xenografts. Neoplasia 2001;3:143-53.
42. Dvorak HF, Brown LF, Detmar M, et al. Vascular permeability factor/vascular endothelial growth factor, microvascular hyperpermeability, and angiogenesis. Am J Pathol 1995;146:1029-39.
43. Folkman J. Tumor angiogenesis: therapeutic implications. N Engl J Med 1971;285:1182-6.
44. Hanahan D, Christofori G, Naik P, et al. Transgenic mouse models of tumour angiogenesis: the angiogenic switch, its molecular controls, and prospects for preclinical therapeutic models. Eur J Cancer 1996;32A:2386-93.
45. Hanahan D, Folkman J. Patterns and emerging mechanisms of the angiogenic switch during tumorigenesis. Cell 1996;86:353-64.
46. Menakuru SR, Brown NJ, Staton CA, et al. Angiogenesis in pre-malignant conditions. Br J Cancer 2008;99:1961-6.
47. Machein MR, Kullmer J, Fiebich BL, et al. Vascular endothelial growth factor expression, vascular volume, and, capillary permeability in human brain tumors. Neurosurgery 1999;44:732-40; discussion 740-1.
48. Raatschen HJ, Simon GH, Fu Y, et al. Vascular permeability during antiangiogenesis treatment: MR imaging assay results as biomarker for subsequent tumor growth in rats. Radiology 2008;247:391-9.
49. Pham CD, Roberts TP, van Bruggen N, et al. Magnetic resonance imaging detects suppression of tumor vascular permeability after administration of antibody to vascular endothelial growth factor. Cancer Invest 1998;16:225-30.
50. Brasch R, Pham C, Shames D, et al. Assessing tumor angiogenesis using macromolecular MR imaging contrast media. J Magn Reson Imaging 1997;7:68-74.
51. Gossmann A, Helbich TH, Kuriyama N, et al. Dynamic contrast-enhanced magnetic resonance imaging as a surrogate marker of tumor response to anti-angiogenic therapy in a xenograft model of glioblastoma multiforme. J Magn Reson Imaging 2002;15:233-40.
52. Batchelor TT, Sorensen AG, di Tomaso E, et al. AZD2171, a pan-VEGF receptor tyrosine kinase inhibitor, normalizes tumor vasculature and alleviates edema in glioblastoma patients. Cancer Cell 2007;11:83-95.
53. Gururangan S, Chi SN, Young Poussaint T, et al. Lack of efficacy of bevacizumab plus irinotecan in children with recurrent malignant glioma and diffuse brainstem glioma: a Pediatric Brain Tumor Consortium study. J Clin Oncol 2010;28:3069-75.
54. Gururangan S, Fangusaro J, Young Poussaint T, et al. Lack of efficacy of bevacizumab + irinotecan in cases of pediatric recurrent ependymoma--a Pediatric Brain Tumor Consortium study. Neuro Oncol 2012;14:1404-12.
55. Blanchette M, Tremblay L, Lepage M, et al. Impact of drug size on brain tumor and brain parenchyma delivery after a blood-brain barrier disruption. J Cereb Blood Flow Metab 2014;34:820-6.
56. Park J, Zhang Y, Vykhodtseva N, et al. The kinetics of blood brain barrier permeability and targeted doxorubicin delivery into brain induced by focused ultrasound. J Control Release 2012;162:134-42.
57. Fortin D, Desjardinsv A, Benko A, et al. Enhanced chemotherapy delivery by intraarterial infusion and blood-brain barrier disruption in malignant brain tumors: the Sherbrooke experience. Cancer 2005;103:2606-15.
58. Kroll RA, Neuwelt EA. Outwitting the blood-brain barrier for therapeutic purposes: osmotic opening and other means. Neurosurgery 1998;42:1083-99; discussion 1099-100.
59. Neuwelt EA, Frenkel EP, Rapoport S, et al. Effect of osmotic blood-brain barrier disruption on methotrexate pharmacokinetics in the dog. Neurosurgery 1980;7:36-43.
60. Zünkeler B, Carson RE, Olson J, et al. Hyperosmolar

blood-brain barrier disruption in baboons: an in vivo study using positron emission tomography and rubidium-82. J Neurosurg 1996;84:494-502.
61. Black KL, Yin D, Ong JM, et al. PDE5 inhibitors enhance tumor permeability and efficacy of chemotherapy in a rat brain tumor model. Brain Res 2008;1230:290-302.
62. Etame AB, Diaz RJ, Smith CA, et al. Focused ultrasound disruption of the blood-brain barrier: a new frontier for therapeutic delivery in molecular neurooncology. Neurosurg Focus 2012;32:E3.
63. Hynynen K. Focused ultrasound for blood-brain disruption and delivery of therapeutic molecules into the brain. Expert Opin Drug Deliv 2007;4:27-35.
64. Liu HL, Yang HW, Hua MY, et al. Enhanced therapeutic agent delivery through magnetic resonance imaging-monitored focused ultrasound blood-brain barrier disruption for brain tumor treatment: an overview of the current preclinical status. Neurosurg Focus 2012;32:E4.
65. Yang FY, Ko CE, Huang SY, et al. Pharmacokinetic changes induced by focused ultrasound in glioma-bearing rats as measured by dynamic contrast-enhanced MRI. PLoS One 2014;9:e92910.
66. Vlachos F, Tung YS, Konofagou EE. Permeability assessment of the focused ultrasound-induced blood-brain barrier opening using dynamic contrast-enhanced MRI. Phys Med Biol 2010;55:5451-66.

Cite this article as: Lam S, Lin Y, Warnke PC. Permeability imaging in pediatric brain tumors. Transl Pediatr 2014;3(3):218-228. doi: 10.3978/j.issn.2224-4336.2014.07.01